Nuclear spin relaxation due to motion on inequivalent sites: H diffusion on O and T sites in the face-centred cubic structure

2003 J. Phys.: Condens. Matter 15 937

(http://iopscience.iop.org/0953-8984/15/6/320)

INSTITUTE OF PHYSICS PUBLISHING JOURNAL OF PHYSICS: CONDENSED MATTER

J. Phys.: Condens. Matter **15** (2003) 937–944 PII: S0953-8984(03)55914-8

Nuclear spin relaxation due to motion on inequivalent sites: H diffusion on O and T sites in the face-centred cubic structure

Xinjun Luo and C A Sholl

Physics and Electronics, University of New England, Armidale, NSW 2351, Australia

Received 11 November 2002
Published 3 February 2003
Online at stacks.iop.org/JPhysCM/15/937

Abstract

Magnetization recoveries for nuclear spin relaxation of like spins due to magnetic dipolar coupling and diffusion on inequivalent sites involve a sum of exponentials. The theory is applied to diffusion on octahedral and tetrahedral interstitial sites in the face-centred cubic structure. Monte Carlo simulations have been used to generate relaxation data for parameters typical for H in metals. It is found that only a single exponential would be observable in the high- and low-temperature limits, but that two-exponential recoveries could be observable in the vicinity of the maximum in the relaxation rate as a function of temperature. The Monte Carlo relaxation data has been fitted using a Bloembergen–Pound–Purcell (BPP) model to assess the accuracy of the BPP model.

1. Introduction

It has been shown by Jaroszkiewicz and Strange (1985) (to be referred to as JS) that the magnetization recoveries for nuclear spin relaxation of like spins due to magnetic dipolar coupling and diffusion on inequivalent sites involve a sum of exponentials. A simpler derivation of the theory has been given by Sholl (1998). The physical origin of the multiexponential recoveries is that spins on crystallographically inequivalent sites experience different fluctuating fields at each type of site and therefore relax at different rates. The magnetic dipolar interactions between spins on equivalent and inequivalent sites, together with the physical diffusion of the spins between the types of site, are taken into account in deriving the relaxation rates and magnetization recoveries. The number of exponentials in the magnetization recoveries is equal to the number of types of inequivalent site.

The theory was applied by JS to analyse relaxation data for the ionic conductor LaF_3 in which the mobile fluorine anions diffuse on several inequivalent sites. In addition to the multiexponential recoveries, the relaxation rates as functions of temperature showed more complex behaviour than the single peak usually observed for diffusion between equivalent sites when the logarithm of the relaxation rate is plotted against reciprocal temperature.

Another example of a single nuclear species diffusing on inequivalent sites is the diffusion of hydrogen in some complex metal–hydrogen systems (Barnes 1997). The present work applies the theory of relaxation for inequivalent sites to the example of hydrogen diffusing on octahedral (O) and tetrahedral (T) sites in the face-centred cubic (FCC) structure. Relevant metal–hydrogen systems are H in transition metals at high H concentrations. The H tend to occupy the T sites at low H concentrations and increasingly occupy the O sites as stoichiometry is approached. An aim is to determine under what circumstances the multiexponential magnetization recoveries would be observable, and whether significant deviations from the simple single peak in the relaxation rate as a function of reciprocal temperature occur. Previous analyses of data for these systems have assumed a single-exponential recovery and relaxation rate.

A second aim of this work is to assess the accuracy of a Bloembergen–Pound–Purcell (BPP) model for analysing the relaxation data for diffusion on O and T systems in the FCC structure. This is accomplished by calculating relaxation rates from Monte Carlo simulations and analysing this data using the BPP model.

The basic structure and diffusion model is described in section 2, the theory of the magnetization recoveries is summarized in section 3 and the details of the relevant spectral density functions, and the BPP model for them, are given in section 4. Results of Monte Carlo simulations of relaxation data and fitting of the data using the BPP model are presented and discussed in section 5.

2. Structure and diffusion model

The O sites in the FCC lattice form an FCC lattice with the same lattice parameter and the T sites form a simple cubic lattice with half the FCC lattice parameter. Each O site has 12 nearest-neighbour O sites and eight nearest-neighbour T sites. Each T site has six nearest-neighbour T sites and four nearest-neighbour O sites. The energies of H at O and T sites are E_{O} and E_{T} (which will be taken as 0), respectively. It will be assumed that diffusion occurs by jumps from O and T sites to neighbouring O and T sites and that the jumps are of Arrhenius form $\Gamma = \Gamma_0 \exp^{-E\beta}$ where $\beta = 1/(kT)$. The jumps are over potential barriers with energies E_{OO}, $E_{\mathrm{OT}} = E_{\mathrm{TO}}$ and E_{TT}. An attempted jump is not successful if the target site is occupied.

The fraction c of the total O and T sites occupied is related to the fractional occupations c_{T} and c_{O} of T and O sites, respectively, by

$$3c = 2c_{\mathrm{T}} + c_{\mathrm{O}} \tag{1}$$

since there are twice as many T sites as O sites. It is assumed that the energy parameters are independent of temperature and the fraction c of occupied sites.

The equilibrium occupation probabilities c_{T} and c_{O} are determined by the rates of transfer between the O and T sites. The number of jumps per second between O and T sites is

$$N_{\mathrm{T}} c_{\mathrm{T}} \Gamma_{\mathrm{TO}} Z_{\mathrm{TO}} (1 - c_{\mathrm{O}}) = N_{\mathrm{O}} c_{\mathrm{O}} \Gamma_{\mathrm{OT}} Z_{\mathrm{OT}} (1 - c_{\mathrm{T}}) \tag{2}$$

where N_{T} is the number of T sites in the system, Γ_{TO} is the rate of attempted jumps from a T site to a particular neighbouring O site, Z_{TO} is the number of O nearest neighbours to a T site, and similarly for the O and T labels interchanged. Therefore

$$\frac{1}{N_{\mathrm{T}} Z_{\mathrm{TO}} \Gamma_{\mathrm{T0}}} \left(\frac{1}{c_{\mathrm{T}}} - 1 \right) \mathrm{e}^{-E_{\mathrm{T}}\beta} = \frac{1}{N_{\mathrm{O}} Z_{\mathrm{OT}} \Gamma_{\mathrm{O0}}} \left(\frac{1}{c_{\mathrm{O}}} - 1 \right) \mathrm{e}^{-E_{\mathrm{O}}\beta} \tag{3}$$

since $\Gamma_{\mathrm{TO}} = \Gamma_{\mathrm{T0}} \exp[-(E_{\mathrm{TO}} - E_{\mathrm{T}})\beta]$ and $\Gamma_{\mathrm{OT}} = \Gamma_{\mathrm{O0}} \exp[-(E_{\mathrm{TO}} - E_{\mathrm{O}})\beta]$. Each side of equation (3) is equal to a function of β, $A(\beta)$, so

$$c_{\mathrm{T}} = \frac{1}{N_{\mathrm{T}} Z_{\mathrm{TO}} \Gamma_{\mathrm{T0}} A(\beta) \mathrm{e}^{E_{\mathrm{T}}\beta} + 1} \qquad c_{\mathrm{O}} = \frac{1}{N_{\mathrm{O}} Z_{\mathrm{OT}} \Gamma_{\mathrm{O0}} A(\beta) \mathrm{e}^{E_{\mathrm{O}}\beta} + 1}. \tag{4}$$

$A(\beta)$ is obtained from equations (1) and (4). If $N_T Z_{TO}\Gamma_{T0} = N_O Z_{OT}\Gamma_{O0}$, the expressions (4) for c_T and c_O are the Fermi–Dirac distribution. For the O and T sites in the FCC structure, $N_T Z_{TO} = N_O Z_{OT}$ and it will be assumed that the prefactors $\Gamma_{T0} = \Gamma_{O0} = \Gamma_0$ so that the fractional occupations of the T and O sites are given by the Fermi–Dirac distribution.

3. Magnetization recoveries and relaxation rates

As shown by JS and Sholl (1998), the components of the magnetizations $M_T(t)$ and $M_O(t)$ of the spins on T and O sites are the solutions of

$$\frac{dM_T}{dt} = -a_{TT}M_T - a_{TO}M_O \qquad \frac{dM_O}{dt} = -a_{OT}M_T - a_{OO}M_O \tag{5}$$

where the time-independent coefficients a_{TT}, a_{TO}, a_{OT} and a_{OO} depend on the spectral density functions of the magnetic dipolar fluctuations and the rates of jumps between O and T sites. The components of magnetization may be the longitudinal or transverse magnetizations in either the laboratory or rotating frames. Only the longitudinal components will be considered in this paper.

The expressions for the coefficients for relaxation in the laboratory frame are

$$a_{TT} = 4\Gamma_{TO}(1 - c_O) + \frac{K}{12}[18J^{(1)}_{TT}(\omega) + 18J^{(2)}_{TT}(2\omega) + J^{(0)}_{TO}(0) + 18J^{(1)}_{TO}(\omega) + 9J^{(2)}_{TO}(2\omega)] \tag{6}$$

$$a_{TO} = -8\Gamma_{OT}(1 - c_T) + \frac{2c_T}{c_O}\frac{K}{12}[-J^{(0)}_{TO}(0) + 9J^{(2)}_{TO}(2\omega)] \tag{7}$$

$$a_{OT} = -4\Gamma_{TO}(1 - c_O) + \frac{c_O}{2c_T}\frac{K}{12}[-J^{(0)}_{OT}(0) + 9J^{(2)}_{OT}(2\omega)] \tag{8}$$

$$a_{OO} = 8\Gamma_{OT}(1 - c_T) + \frac{K}{12}[18J^{(1)}_{OO}(\omega) + 18J^{(2)}_{OO}(2\omega) + J^{(0)}_{OT}(0) + 18J^{(1)}_{OT}(\omega) + 9J^{(2)}_{OT}(2\omega)] \tag{9}$$

where $K = \gamma^4\hbar^2 I(I + 1)$, γ is the gyromagnetic ratio of a spin, I is the quantum number of the spin, $\omega = \gamma B_0$ is the resonant frequency of a spin in the applied magnetic field B_0 and $J^{(p)}_{\alpha\beta}(\omega)$ are spectral density functions which are described in the following section.

For relaxation in the rotating frame, the corresponding coefficients are obtained by replacing the spectral density functions $J^{(p)}(p\omega)$ by $J^{(p)}(\omega_1, \omega)$ where

$$J^{(0)}(\omega_1, \omega) = \tfrac{1}{4}J^{(0)}(0) + \tfrac{9}{8}J^{(2)}(2\omega) \tag{10}$$

$$J^{(1)}(\omega_1, \omega) = \tfrac{1}{2}J^{(1)}(\omega) + \tfrac{1}{8}J^{(2)}(2\omega) \tag{11}$$

$$J^{(2)}(\omega_1, \omega) = \tfrac{1}{4}J^{(0)}(2\omega_1) + 2J^{(1)}(\omega) + \tfrac{1}{8}J^{(2)}(2\omega) \tag{12}$$

and $\omega_1 = \gamma B_1$ is the resonant frequency in the rotating field B_1.

The solution of the differential equations (5) shows that each of $M_T(t)$ and $M_O(t)$ are linear combinations of two exponentials. The observed magnetization is $M(t) = M_T(t) + M_O(t)$ and

$$M(t) = U\exp(-\lambda_+ t) + V\exp(-\lambda_- t) \tag{13}$$

where

$$\lambda_\pm = (a_{TT} + a_{00} \pm f)/2 \tag{14}$$

$$U = [(a_{TT} + a_{OT} - \lambda_-)M_T(0) + (a_{TO} + a_{OO} - \lambda_-)M_O(0)]/f \tag{15}$$

$$V = [(\lambda_+ - a_{TT} - a_{OT})M_T(0) + (\lambda_+ - a_{TO} - a_{OO})M_O(0)/f \tag{16}$$

$$f = [(a_{TT} - a_{OO})^2 + 4a_{TO}a_{OT}]^{1/2}. \tag{17}$$

The initial condition for the magnetization satisfies $2c_T M_O(0) = c_O M_T(0)$ since the initial magnetizations are proportional to the populations of the T and O sites.

Magnetization recoveries for spins diffusing on equivalent sites have single-exponential recoveries. For longitudinal relaxation the relaxation rate is (Abragam 1961)

$$R_1 = \frac{3K}{2}[J^{(1)}(\omega) + J^{(2)}(2\omega)]. \tag{18}$$

It is interesting to develop this expression for inequivalent sites by assuming that the spectral density functions are the weighted averages for the various O and T dipolar interactions. The result is

$$R_1 = \frac{3K}{2}\left\{\frac{2c_\mathrm{T}}{3c}[J^{(1)}_\mathrm{TT}(\omega) + J^{(2)}_\mathrm{TT}(2\omega) + J^{(1)}_\mathrm{TO}(\omega) + J^{(2)}_\mathrm{TO}(2\omega)] + \frac{c_\mathrm{O}}{3c}[J^{(1)}_\mathrm{OT}(\omega) + J^{(2)}_\mathrm{OT}(2\omega) + J^{(1)}_\mathrm{OO}(\omega) + J^{(2)}_\mathrm{OO}(2\omega)]\right\}. \tag{19}$$

It can be shown that the expression (14) for λ_- reduces to this result for R_1 in both the high- and low-temperature limits.

In the high-temperature limit, the terms $\Gamma_{\alpha\beta}$ dominate the spectral density function terms on the right-hand sides of equations (6)–(9). In this case $\lambda_+ = 4\Gamma_\mathrm{TO}(1 - c_\mathrm{O}) + 8\Gamma_\mathrm{OT}(1 - c_\mathrm{T})$ and λ_- is a much smaller term dependent only on the spectral density functions. Evaluating λ_-, U and V to first order in the spectral density function terms shows that $V \gg U$ and that $\lambda_- = R_1$.

In the low-temperature limit, the terms $\Gamma_{\alpha\beta}$ are negligible and the terms $J^{(0)}_\mathrm{OT}(0)$ and $J^{(0)}_\mathrm{TO}(0)$ dominate the other spectral density functions. Evaluating $\lambda_\pm$, U and V to first order in these terms again shows that $V \gg U$, $\lambda_- = R_1$ and $\lambda_+ = K[J^{(0)}_\mathrm{OT}(0) + J^{(0)}_\mathrm{TO}(0)]/12$. It follows that only a single-exponential recovery described by λ_- would be observable in both the high- and low-temperature limits, and that λ_- is then given by R_1.

4. Spectral density functions and BPP models

The spectral density functions $J^{(p)}(\omega)$ are the Fourier transforms of the correlation functions $G^{(p)}(t)$ of the fluctuations of magnetic dipolar interactions between pairs of diffusing spins. For inequivalent sites they are (JS)

$$G^{(p)}_{\alpha\beta}(t) = \sum_{\boldsymbol{x}} \sum_{\boldsymbol{r}_0 \neq 0} \sum_{\boldsymbol{r}(\beta)\neq 0} c_\beta u^{(p)}(\boldsymbol{r}_0) u^{(-p)}(\boldsymbol{r}) P(\boldsymbol{x}, \boldsymbol{0}; t) P(\boldsymbol{x} + \boldsymbol{r}_0, \boldsymbol{r}; t) \tag{20}$$

where α and β are O or T, the sums over $\boldsymbol{x}$ and $\boldsymbol{r}_0$ are over all crystal sites, the sum over $\boldsymbol{r}$ is over all β-sites and the origin is an α-site. The function $P(\boldsymbol{x}, \boldsymbol{y}; t)$ is the probability of a spin being at $\boldsymbol{y}$ at time t given that it was at $\boldsymbol{x}$ at time zero, and c_β is the fractional concentration of spins on β-sites. The function $u^{(p)}(\boldsymbol{r}) = d_p^2 Y_{2p}(\Omega)/r^3$ where Y_{2p} are spherical harmonics relative to the direction of the magnetic field as the z-axis, and $d_0^2 = 16\pi/5$, $d_1^2 = 8\pi/15$ and $d_2^2 = 32\pi/15$. The correlation function is for relaxation of a spin i at the origin at time t interacting with a spin j at $\boldsymbol{r}$ at time t, averaged over all possible starting positions of the spins at time 0. For the spherical average over magnetic field directions appropriate for polycrystalline samples, the term $u^{(p)}(\boldsymbol{r}_0)u^{(-p)}(\boldsymbol{r})$ is replaced by $(2C_p/15)P_2(\cos\theta)/(r^3 r_0^3)$ where θ is the angle between $\boldsymbol{r}$ and $\boldsymbol{r}_0$, and $C_0 = 6$, $C_1 = 1$ and $C_2 = 4$ (Sholl 1974).

A BPP model for the correlation function assumes that the correlation is destroyed when a jump of either of a pair of interacting spins occurs. The BPP correlation function is therefore

$$G^{(p)}_{\alpha\beta}(t) = c_\beta \sum_{\boldsymbol{r}(\beta)\neq 0} |u^{(p)}(\boldsymbol{r})|^2 \mathrm{e}^{-(\Gamma_\alpha + \Gamma_\beta)t} = c_\beta C_p S_{\alpha\beta} \mathrm{e}^{-(\Gamma_\alpha + \Gamma_\beta)t} \tag{21}$$

where the exponential is the probability of no jump of either spin in a time t, Γ_α is the total rate of jumps away from an α-site, and $S_{\alpha\beta} = \sum_{r(\beta)\neq 0} 1/r^6$ with the origin at an α-site. The expressions for Γ_α are

$$\Gamma_T = 6\Gamma_{TT}(1 - c_T) + 4\Gamma_{TO}(1 - c_O) \qquad \Gamma_O = 12\Gamma_{OO}(1 - c_O) + 8\Gamma_{OT}(1 - c_T). \tag{22}$$

A simpler BPP model would assume that $\Gamma_\alpha = \Gamma_0 e^{-E\beta}$ independent of the type of site, where Γ_0 and the energy E are fitting parameters, but this has not been considered.

The spectral density functions were calculated by Monte Carlo simulations to provide an accurate basis for comparison of the BPP models. The simulations used 6^3 FCC unit cells. A continuous time method was used to obtain the correlation functions and it was verified that the correlation functions were proportional to $t^{-3/2}$ in the long-time limit as an aid to obtaining accurate spectral density functions (Luo and Sholl 2002).

5. Results

Calculations were performed for some typical values of parameters for H in metals (Majer *et al* 1994) in order to determine the types of effect that could be observed and to test the accuracy of the BPP model. Two sets of parameters were used. For both sets of parameters, $\Gamma_0 = 10^{13}$ Hz for all jump prefactors, $E_T = 0$ eV, $E_{TT} = 0.5$ eV, $E_{TO} = 0.9$ eV, $E_{OO} = 0.6$ eV, and the resonant frequency is 60 MHz. Pairs of values of E_O and c were chosen to give different proportions of O- and T-site occupancies. One set has $E_O = 0.22$ eV and $c = 0.667$ and the other set has $E_O = 0.1$ eV and $c = 0.62$.

Results of the Monte Carlo simulations for the temperature dependence of $\lambda_\pm$ are shown for the two sets of parameters in figures 1 and 2. Also shown are the results for R_1 from equation (19) and the high- and low-temperature limits for λ_+ as discussed in section 3. The units of $\lambda_\pm$ and R_1 are $3KSc/(5a^6)$ where $a = 2.5$ nm. The insets in the figures show the corresponding temperature dependences of the occupation probabilities of the O and T sites as calculated from equation (4). The parameters used in figure 2 result in mainly T-site occupation of the spins, while the parameters used in figure 1 give more O-site occupancy. It can be seen that the expression for R_1 is an excellent approximation to λ_- in the high- and low-temperature limits but is less satisfactory in the vicinity of the maximum in λ_-.

The two magnetization recovery exponents $\lambda_\pm$ are greatly different, except in the vicinity of the maximum of λ_- where both curves show structure unlike the smooth maxima in the corresponding relaxation rate curves for simple systems. By comparing figures 1 and 2 it is apparent that this structure in the curves is greater and the two exponents are closer in magnitude, for sets of parameters which give more equal occupancy of the inequivalent O and T sites.

The observable magnetization recoveries given by equation (13) involve the coefficients U and V given by equations (15) and (16). The temperature dependence of the ratio U/V is shown for both sets of parameters in figure 3. The values of U/V are very small except near the maxima in λ_-, so in the high- and low-temperature limits away from these maxima only a single-exponential magnetization recovery characterized by λ_- would be observable. Examples of magnetization recoveries where two exponentials might be observed experimentally are shown in figure 4. In such cases it would be useful to deduce both exponents $\lambda_\pm$ and the value of U/V from the experimental data.

Fits of the BPP model given by equation (21) to the Monte Carlo data in figures 1 and 2 are shown in figure 5. The results shown are for least-squares fits obtained by varying Γ_0 and all the energy parameters except E_T. The fit value of $\Gamma_0 = 10^{13}$ Hz is the same as for the Monte Carlo data. The fit values of the energy parameters are as follows, where the figures in parentheses

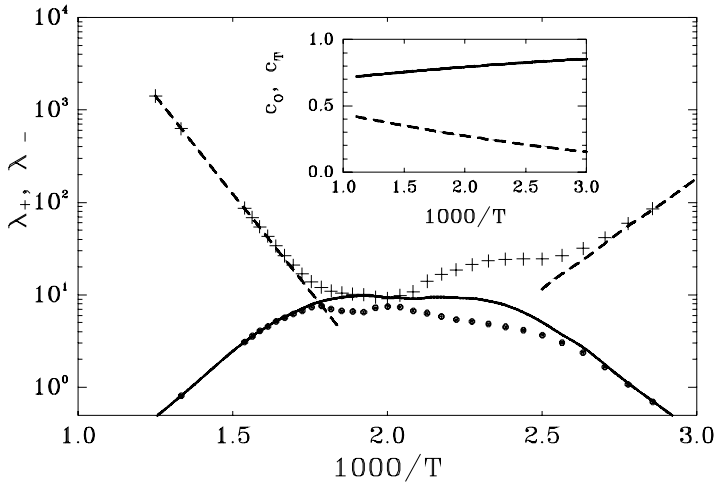

Figure 1. Values of the exponents $\lambda_\pm$ (+ and ● symbols) as a function of $1000/T$ for the $c = 0.62$ parameters. The solid curve shows the values of R_1 in equation (19) and the dashed lines are the high- and low-temperature limits of λ_- as described in the text. The inset shows the values of the occupation probabilities c_O and c_T of the O and T sites as a function of $1000/T$.

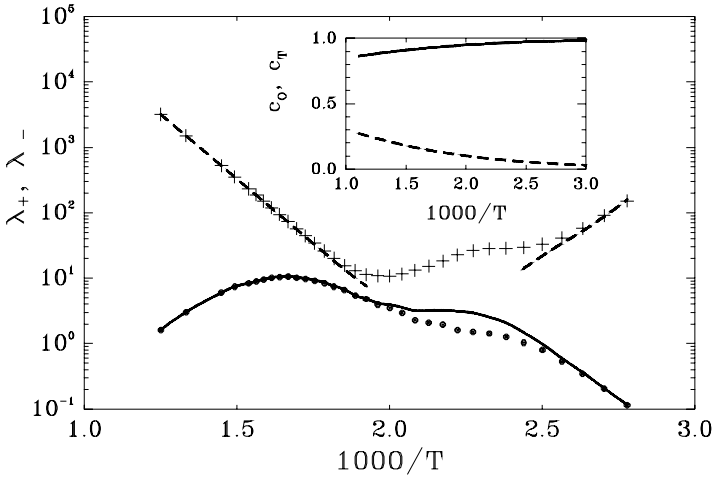

Figure 2. As figure 1, but for the $c = 0.667$ parameters.

are the original Monte Carlo parameters. For the $c = 0.667$ data, $E_O = 0.20$ (0.22) eV, $E_{TT} = 0.55$ (0.5) eV, $E_{TO} = 0.89$ (0.9) eV, $E_{OO} = 0.70$ (0.6) eV, and for the $c = 0.62$ data, $E_O = 0.08$ (0.1) eV, $E_{TT} = 0.54$ (0.5) eV, $E_{TO} = 0.90$ (0.9) eV, $E_{OO} = 0.56$ (0.6) eV. The corresponding results for U/V for the fit parameters are shown in figure 3. The quality of the fit to the $\lambda_\pm$-data is excellent for both sets of parameters. The energy parameters deduced from the fit agree with the input energies to typically within 10%. The BPP model therefore provides an acceptable model for analysing such data within these limits of accuracy.

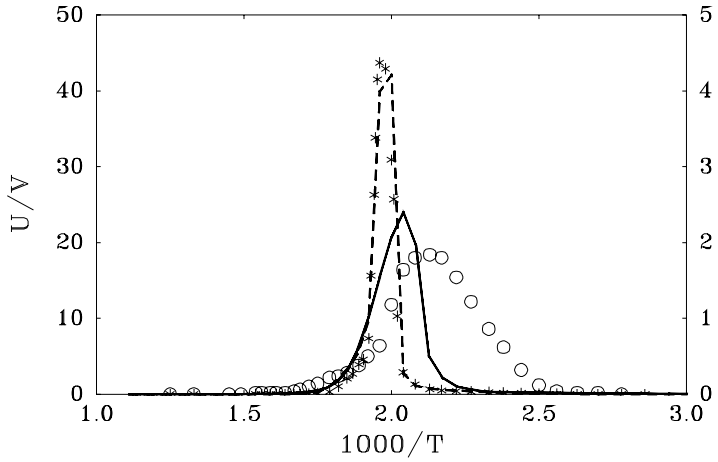

Figure 3. Values of the ratio U/V of the coefficients of the exponentials for the magnetization recoveries in equation (13) as a function of $1000/T$. For the $c = 0.62$ parameters, the $*$ symbols show the Monte Carlo values and the dashed curve shows the BPP results (left-hand scale). For the $c = 0.667$ parameters, the circle symbols show the Monte Carlo values and the solid curve shows the BPP results (right-hand scale).

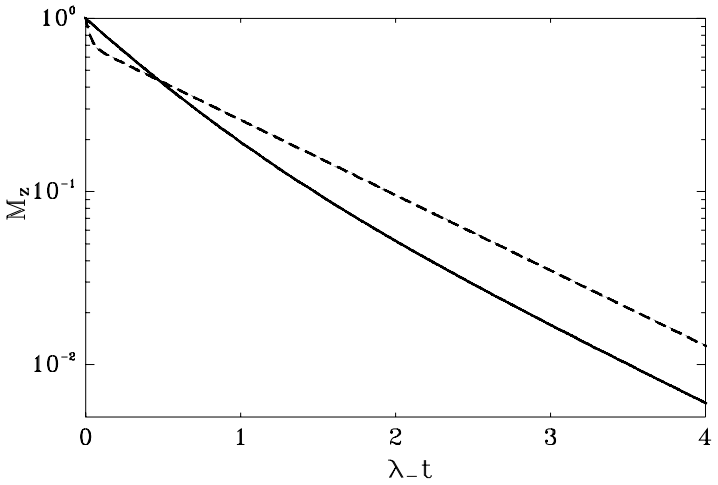

Figure 4. Magnetization recoveries for $1000/T = 2$. The solid curve is for the $c = 0.62$ parameters and the dashed curve is for the $c = 0.667$ parameters.

6. Conclusions

Nuclear spin magnetization recoveries are sums of exponentials for relaxation due to diffusion between inequivalent sites. The example of diffusion between O and T sites in the FCC structure considered here shows that the multiexponential recoveries will not always be observable because the coefficient of one of the exponentials will be negligible, or because one of the exponents will be very large. When only one exponential can be observed it will be the one corresponding to the smaller of the two exponents. Multiexponential recoveries are most likely to be observed at temperatures corresponding to the maximum in the recovery rate. The observation of multiexponential behaviour in such circumstances would provide strong

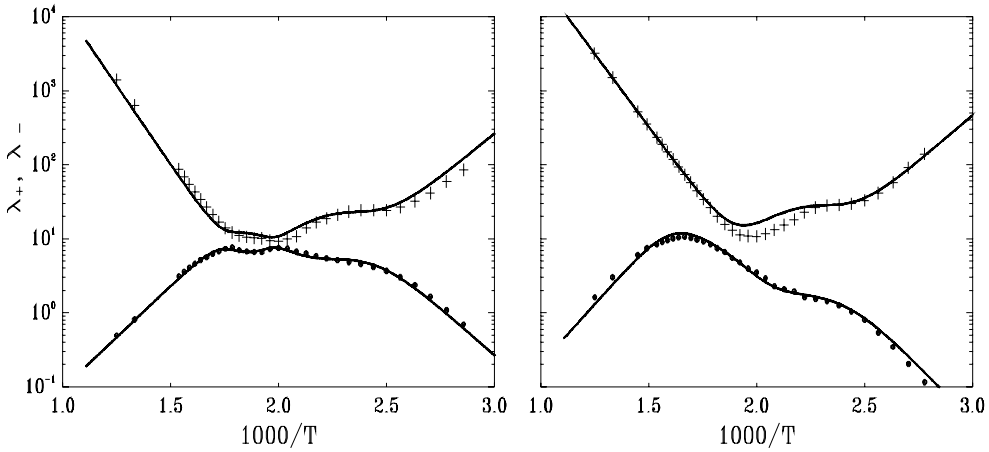

Figure 5. Fits of the BPP model (curves) to the Monte Carlo results for $\lambda_{\pm}$. The left-hand figure is for the $c = 0.62$ parameters and the right-hand figure is for the $c = 0.667$ parameters.

evidence for diffusion between inequivalent sites when the relaxation mechanism is due to magnetic dipolar interactions. The additional recovery exponent observed and the ratio of the coefficients of the exponentials also provides further data to assist in understanding the diffusion behaviour.

The analysis of relaxation data using Monte Carlo simulations is very time-consuming and the use of a BPP model is a much simpler approach. The comparison of the BPP model results with the Monte Carlo simulation data in the previous section has shown the type of quality of fit that can be expected from a least-squares fit to experimental data and the accuracy of the deduced parameters.

The theory presented here could be extended straightforwardly to the inclusion of the effect of metal–hydrogen interactions where these dipolar interactions were significant, to longitudinal relaxation in the rotating frame and transverse relaxation, and to other complex H–metal systems such as diffusion between e and g sites in Laves phase materials.

References

Abragam A 1961 *Principles of Nuclear Magnetism* (Oxford: Clarendon) p 291
Barnes R G 1997 *Top. Appl. Phys.* **73** 93
Jaroszkiewicz G A and Strange J H 1985 *J. Phys. C: Solid State Phys.* **18** 2331
Luo X and Sholl C A 2002 *J. Phys.: Condens. Matter* **14** 6941
Majer G, Renz W and Barnes R G 1994 *J. Phys.: Condens. Matter* **6** 2935
Sholl C A 1974 *J. Phys. C: Solid State Phys.* **7** 3378
Sholl C A 1998 *J. Phys.: Condens. Matter* **10** 3255